Zero *g* factors and nonzero orbital momenta in self-assembled quantum dots

Weidong Sheng
Department of Physics, Fudan University, Shanghai 200433, China
and Institute for Microstructural Sciences, National Research Council, Ottawa, Ontario, Canada K1A 0R6

A. Babinski
Institute of Experimental Physics, Warsaw University, Hoza 69, 00-681 Warszawa, Poland
(Received 8 December 2006; published 26 January 2007)

We point out using an empirical tight-binding approach that the ground state of holes in InAs/GaAs self-assembled quantum dots carries nonzero orbital momentum. The spin and orbital motions of the hole state are found to have opposite contributions to the hole *g* factor, leading to zero *g* factors of holes and then excitons in dots of high aspect ratio. The nonzero envelope orbital momenta of the holes are also shown to account for anisotropic circular polarization of exciton emission and nonlinear Zeeman splittings in high magnetic fields. Our theory well explains recent experiments and indicates the possibility of engineering magnetic splitting by tuning the electric confinement in nanostructures.

DOI: 10.1103/PhysRevB.75.033316 PACS number(s): 71.18.+y, 78.67.Hc, 73.21.La

As one of the most important magnetic properties of a system, the *g* factor measures the Zeeman splitting of an electron state in a magnetic field and is determined by both the spin and orbital motion of the electron. In semiconductors like InAs and GaAs, the orbital motion of localized *p* orbitals is strongly coupled to the spin, and the resulting valence-band states can be classified by the corresponding total angular momentum. Heavy and light holes, identified by their different angular momenta, have distinctive *g* factors, i.e., $g_{hh}^{s}=-6\kappa$ and $g_{lh}^{s}=-2\kappa$ where κ is an empirical parameter in the $k\cdot p$ theory.[1]

In addition to the orbital motion of localized atomic orbitals, electrons in nanostructures like self-assembled quantum dots[2] can also acquire orbital magnetic moment due to the motion around the circumference of the structures. However, it is often taken for granted that the ground state of a single exciton in these artificial atoms does not carry any nonzero orbital momenta largely because the lowest level of a natural atom is known to always have zero orbital momentum. Such ignorance of the orbital motion can greatly impede the understanding of electron and hole *g* factors in quantum dots.[3]

While it is true that the ground state of electrons in quantum dots does not carry any angular momentum, we find that the ground state of holes does carry nonzero envelope angular momenta. In the present work, we will show that the nonzero envelope orbital momenta (NEOM) of holes is essential to understand the behavior of *g* factors of holes and excitons and can explain the zero exciton *g* factor and nonlinear Zeeman splittings observed in a recent experiment. Moreover, we predict that the NEOM would lead to anisotropic circular polarization of the exciton emission.

For the purpose of this study, we choose an sp^3 tight-binding method[4] which has been successfully applied in ferromagnetic quantum wells.[5] The one-electron tight-binding Hamiltonian describes an electron hopping from atomic spin orbital (α,σ) at position $\mathbf{R}$ to spin orbital (α',σ') at position $\mathbf{R}'$:

$$H_{tb}=\sum_{\mathbf{R},\alpha,\sigma,\mathbf{R}',\alpha',\sigma'} H(\mathbf{R},\alpha,\sigma;\mathbf{R}',\alpha',\sigma')c^{\dagger}_{\mathbf{R},\alpha,\sigma}c_{\mathbf{R}',\alpha',\sigma'}, \tag{1}$$

where $c^{\dagger}_{\mathbf{R},\alpha,\sigma}$ ($c_{\mathbf{R}',\alpha',\sigma'}$) are creation (annihilation) operators. The basis of the spin orbitals is chosen as $\{|s_{\downarrow}\rangle,|x_{\downarrow}\rangle,|y_{\downarrow}\rangle,|z_{\downarrow}\rangle,|s_{\uparrow}\rangle,|x_{\uparrow}\rangle,|y_{\uparrow}\rangle,|z_{\uparrow}\rangle\}$. The hopping matrix elements and site energies for *s* and *p* orbitals are extended to include second-nearest-neighbor interactions[6] to fit the effective masses of electrons and holes at the Γ point and conduction- and valence-band edges at both the Γ and *X* points exactly. Spin-orbit interaction is also incorporated.

In a magnetic field, Peierls phase factors are introduced to transform the off-diagonal matrix elements as

$$H(\mathbf{R},\mathbf{R}')\rightarrow \exp\left(-i\frac{e}{\hbar}\int_{\mathbf{R}}^{\mathbf{R}'}\mathbf{A}(\mathbf{r})d\mathbf{r}\right)H(\mathbf{R},\mathbf{R}'), \tag{2}$$

where $\mathbf{A}(\mathbf{r})$ is the vector potential. The Zeeman effect is included by adding the spin terms to the diagonal matrix elements,

$$H(\mathbf{R}_{\uparrow(\downarrow)},\mathbf{R}_{\uparrow(\downarrow)})\rightarrow H(\mathbf{R}_{\uparrow(\downarrow)},\mathbf{R}_{\uparrow(\downarrow)})\pm\frac{1}{2}g\mu_B B_z, \tag{3}$$

where *g* is the *g* factor of a bare electron. It is noted that no additional empirical parameters like κ are used for the Zeeman effect.

The calculations of electron and hole *g* factors are performed for a typical lens-shaped InAs/GaAs quantum dot which is 20 nm long in diameter, on a 2 monolayer wetting layer and has a varying height. The total number of atoms included in the calculation is about 500 000. A Lanczos algorithm is used to compute the eigenvalues and eigenvectors of large sparse matrices generated by the tight-binding Hamiltonian. The calculation is first performed for the strain distribution by an atomistic valence-force-field method, followed by an analysis of the electronic structure by the tight-binding method.

 ©2007 The American Physical Society

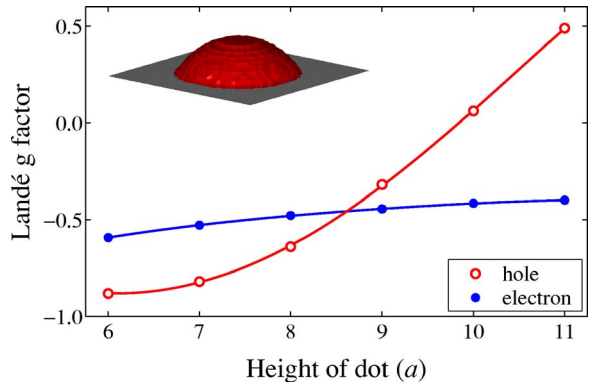

FIG. 1. (Color online) The Landé g factors of holes and electrons, calculated as a function of the height of the lens-shaped self-assembled InAs/GaAs quantum dots as shown in the inset. The heights of the dots are in units of the lattice constant of GaAs.

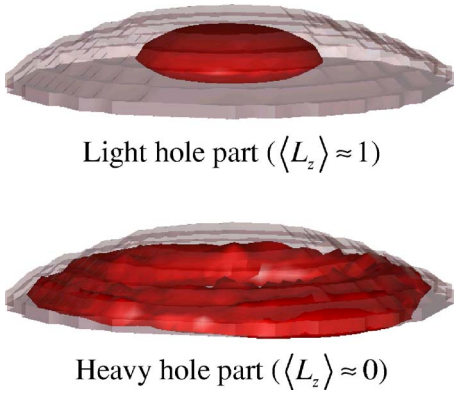

FIG. 2. (Color online) Plots of light and heavy hole envelope functions in the ground state of holes in a flat lens-shaped InAs/GaAs quantum dot. The expectation values of the orbital momentum operator L_z are labeled.

Figure 1 plots the calculated hole and electron g factors, g_h and g_e, as a function of the height of the dots. The result exhibits a weak dependence of the electron g factor on the height of the dots (H). However, the hole g factor is found to increase rapidly as the height H becomes larger. The combined exciton g factor, $g_{ex}=g_h+g_e$, is seen to change from -1.47 when $H\approx 3.4$ nm to 0.09 when $H\approx 6.2$ nm. Hence, the exciton g factor vanishes at a point between $10a$ and $11a$. In a recent magnetospectroscopy experiment of on single InAs/GaAs quantum dots,[7] the exciton g factors of two single dots were measured; one was about 3 nm high and had $g_{ex}=-1.5$ and the other was about 5 nm high and had an almost zero exciton g factor, which nearly quantitatively agrees with our theoretical calculation.

In the following, we will explain why the g factor of holes and then excitons would vanish as the height of the dots increases. Let us start with an analysis of valence-band states in self-assembled quantum dots. Because of the influence of the band mixing and strain field, the valence-band states in quantum dots are much more complex than those in the conduction bands. In general, a hole state in quantum dots is composed of components from the heavy (hh), light (lh), and split-off (sh) hole bands, and the conduction bands (s). It can be written as $\Psi=\Sigma_n \psi_{n\uparrow}|n_\uparrow\rangle+\psi_{n\downarrow}|n_\downarrow\rangle$, where $n=\{hh,lh,sh,s\}$.[8–10] If only the contribution from the Bloch functions is taken into account, the hole g factor can then be expressed as $g_h^s=\Sigma_n g_n(c_{n\uparrow}-c_{n\downarrow})$, where g_n is the g factor for band n and $c_n=|\langle\psi_n|\psi_n\rangle|^2$.[11] Considering that the ground state of the holes is dominated by its heavy and light hole components, we have $g_h^s\approx g_{hh}^s c_{hh\uparrow}+g_{lh}^s c_{lh\uparrow}$. It gives us a simple theory to explain why the hole g factor becomes smaller when the proportion of the heavy hole component decreases,[12] which has been quite successful in quantum wells where the lateral motion of carriers is not confined. However, in quantum dots with strong lateral confinement, understanding of the hole g factor would nevertheless require knowledge of the spatial distribution of the envelope functions of both heavy and light hole components.

Figure 2 plots the probability density of the light ($|\psi_{lh\uparrow}|^2$) and heavy ($|\psi_{hh\uparrow}|^2$) hole components in the ground state of the holes in a dot of $H=6a$. The expectation value of the orbital momentum operator in the envelope functions of the light and heavy hole components can be calculated by $\langle\hat{L_z}\rangle=\langle\psi_h|x(\partial/\partial y)-y(\partial/\partial x)|\psi_h\rangle$. Similar to the ground state of the electrons, we find that the orbital momentum of the dominant heavy hole component is very small ($\langle L_z\rangle<0.01$). However, the light hole components are found to carry nonzero angular momenta, i.e., $\langle L_z\rangle=0.99$ for $\psi_{lh\uparrow}$ and $\langle L_z\rangle=1.79$ for $\psi_{lh\downarrow}$.

The reason why the heavy hole component of zero angular momentum mixes with the light hole parts of nonzero angular momenta lies in the fact that the total angular momentum, i.e., the envelope part plus the Bloch part (L_z+j_z), is a good quantum number in a system with cylindrical symmetry.[8,9,13,14] Even if the symmetry is broken by the shear strain, we find that the conservation of the total angular momentum is still a good approximation.

Including the contribution from the envelope functions, we have the overall hole g factor

$$g_h = g_h^s + g_h^o, \tag{4}$$

where g_h^o denotes the contribution from NEOM,

$$g_h^o = 2\sum_n \langle\psi_{n\uparrow}|\hat{L_z}|\psi_{n\uparrow}\rangle + \langle\psi_{n\downarrow}|\hat{L_z}|\psi_{n\downarrow}\rangle. \tag{5}$$

In the dot of flat shape as shown in Fig. 2, the light hole components have a very small projection in the ground state of holes, i.e., $c_{lh\uparrow}=1.86\%$ and $c_{lh\downarrow}=0.41\%$; hence NEOM give only a small contribution to the hole g factor. As the light hole components take a larger proportion, the contribution from the envelope part becomes more important to the hole g factor.

Figure 3 plots the envelope orbital momenta of the heavy and light hole components, i.e., $\langle\psi_{hh\uparrow}|\hat{L_z}|\psi_{hh\uparrow}\rangle/c_{hh\uparrow}$ and $\langle\psi_{hh\uparrow}|\hat{L_z}|\psi_{lh\uparrow}\rangle/c_{lh\uparrow}$, and g_h^o, as a function of the height of dots. As the aspect ratio of the dot increases, the light hole component is found to have a larger projection ($c_{lh\uparrow}+c_{lh\downarrow}$) in the ground state of holes due to its stronger mixture with the

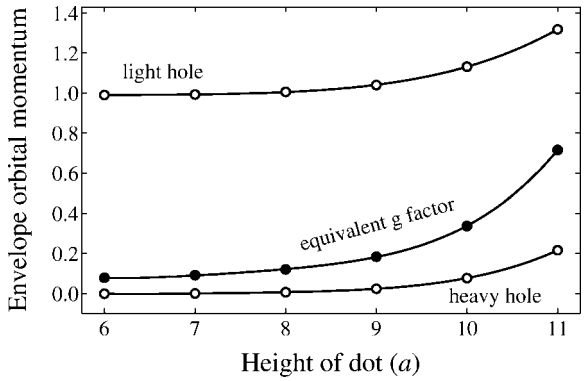

FIG. 3. Envelope orbital momenta of the heavy and light hole components in the ground state of holes and the corresponding equivalent g factor calculated as a function of the height of the lens-shaped self-assembled InAs/GaAs quantum dot as shown in the inset of Fig. 1.

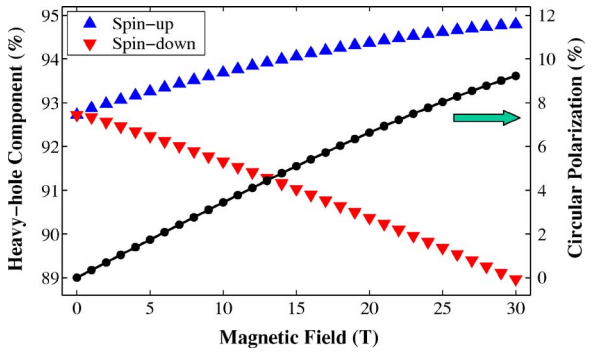

FIG. 4. (Color online) The proportion of the heavy hole component in the spin-up and spin-down states of the holes and the circular polarization of the exciton emission, calculated as a function of magnetic field in a lens-shaped InAs/GaAs quantum dot.

heavy hole part.[12] For example, when the height of the dot (H) changes from $6a \approx 3.4$ nm to $11a \approx 6.2$ nm where a is the lattice constant of GaAs, $c_{lh\uparrow}+c_{lh\downarrow}$ increases from 2.0% to 7.1%; in the meantime, the proportion of the heavy hole part $c_{hh\uparrow}+c_{hh\downarrow}$ drops from 96.6% to 89.0%.

Corresponding to these changes, the equivalent g factor due to NEOM, g_h^o, becomes larger. Moreover, the heavy hole component starts to gain noticeable NEOM when $H>8a$, which gives a significant contribution to g_h^o. For example, the contribution from the heavy hole part alone accounts for 41% of g_h^o when $H=9a$ while it increases to 61% when $H=11a$. When the dot is flat, we find that the contribution from NEOM (g_h^o) is small and the hole g factor is dominated by that from the Bloch parts (g_h^s). In this case, we have $|g_h^o| \ll |g_h^s|$ while $g_h^s<0$ and $g_h^o>0$. With the increase of the aspect ratio of the dot, g_h^o becomes larger because of not only the larger proportion of the light hole component but also the NEOM of the heavy hole parts.

As the aspect ratio of the dot increases, the contribution from the Bloch parts (g_h^s) is seen to become smaller while that from the envelope orbital momenta (g_h^o) becomes the dominant part in the hole g factor. Because the two parts (g_h^s and g_h^o) have the opposite signs, they are found to nearly cancel each other when $H=10a$, which results in an almost zero hole g factor. When the aspect ratio increases further, $|g_h^o|$ becomes larger than $|g_h^s|$, which leads to the change of the sign of the overall hole g factor. At $H=11a$, the hole g factor is found to become positive and nearly cancel the electron g factor, leading to an almost zero exciton g factor, which well explains the zero exciton g factor observed in the recent experiment.[7]

While the result shown in Fig. 2 may also be obtained by the eight-band $k\cdot p$ method,[15] we find that it is necessary to apply the tight-binding approach for the calculation of the g factors. The key to this issue is that the κ parameter used in the $k\cdot p$ theory is not well established. Even in quantum wells, a fitting procedure is often required to reproduce the experimental data,[16] and xxx the uncertainty in its value can be as large as 10%. In our $k\cdot p$ calculation, a mere 3% change in κ (from 7.68 to 7.48) can induce a change of more than 20% in the resulting hole g factor (from 0.30 to 0.24). Another difficulty we encounter in the $k\cdot p$ calculation is that in most cases it gives electron and hole g factors with opposite signs,[12] which is in an obvious contradiction with the experiment where the electron and hole g factors are shown to have the same sign.[3]

Besides the zero g factors of holes and excitons, the interplay between the contributions from the Bloch and envelope parts (g_h^s and g_h^o) can lead to many other observable effects such as anisotropic circular polarization of the exciton emission in a high magnetic field. Let us take the example of the dot with height $H=10a$. As can be seen in Fig. 1, the overall hole g factor nearly vanishes due to the opposite contribution from the heavy and light hole parts. It can be estimated that the effective g factor (including both the Bloch parts and NEOM) for the heavy hole part is $g_{hh} \approx -0.07$ and for the light hole part $g_{lh} \approx 0.08$. As the magnetic field increases, the heavy hole part of the spin-up state tends to lower its energy because $g_{hh}<0$. In the meantime, its light hole part tends to do the opposite since $g_{lh}>0$. The competition means that the spin-up state gains more heavy hole part while losing the light hole part as the field increases. A similar process also goes on in the spin-down state, but, ending with the opposite dependence.

The calculated $c_{hh\uparrow}$ and $c_{hh\downarrow}$ are plotted as a function of the magnetic field in Fig. 4, and exhibit the predicted dependence. As the intensity of the σ^+ (σ^-) transition is mainly determined by the proportion of the heavy hole components in the spin-up (spin-down) hole state, the polarized heavy hole components directly lead to the anisotropic circular polarization of the exciton emission. The calculated degree of circular polarization defined[17] by $p=(I_{\sigma^+}-I_{\sigma^-})/(I_{\sigma^+}+I_{\sigma^-})$ is plotted in Fig. 4, and is seen to increase with the magnetic field. It is noted that due to the spin relaxation effect, this phenomenon may not be well resolved when linearly polarized excitation is applied. Instead, circularly polarized excitation should be used for the observation of this effect.

Another observable phenomenon induced by NEOM is nonlinear Zeeman splittings. As the spin-down state is noticed to lose its heavy hole component faster than the spin-up state gains the heavy hole component, the total projection of the heavy hole components in the spin-up and spin-down

hole states decreases as the magnetic field increases, which causes the g factor of holes to change as the magnetic field increases and leads to weak yet observable nonlinear Zeeman splittings.[7]

NEOM also exist in other kinds of systems like carbon nanotubes.[18] Although the motion of carriers is not confined in the lateral directions in quantum wells, a magnetic field applied along the growth direction would induce lateral orbital motion that mixes heavy and light hole states. Such a band mixture sometimes leads to strong nonlinear Zeeman splitting.[16] In spite of some similarities between the orbital motion in quantum dots discussed here and that induced by the applied magnetic field in quantum wells, the difference is obvious: NEOM in self-assembled quantum dots are induced by the structural confinement and hence represent an intrinsic property that does not depend on an external field. While it may be argued that the mechanism leading to NEOM has been included in previous work,[12] we would like to remind the reader that NEOM have not been explicitly studied, let alone their effect on the g factor of holes in quantum dots. On the contrary, it has recently been reported that the behavior of the hole g factor in quantum dots can be understood in terms of orbital momentum quenching,[19] which is proved incorrect by our calculation.

As a result of NEOM, the light hole component in the ground state of holes has almost zero overlap with the ground state of electrons in a flat quantum dot; therefore, it has little contribution to the interband transition. As the aspect ratio increases, $\Delta L_z = \langle \psi_{lh} | L_z | \psi_{lh} \rangle - \langle \psi_e | L_z | \psi_e \rangle$ starts to deviate from 1, which partially lifts the forbidden transition.

In conclusion, we find that the hole g factor has two distinct contributions in self-assembled quantum dots, one from the Bloch functions and the other from the nonzero orbital momenta carried in the envelope functions of the holes. We show that these two contributions to the hole g factor have opposite signs and account for the zero g factors of holes and excitons in dots of high aspect ratio. We also point out that the nonzero orbital momenta are responsible for anisotropic circular polarization of the exciton emission and nonlinear Zeeman splittings.

This work is supported by the NSFC (Nos. 10644001 and 10634040). The authors thank P. Hawrylak and M. Korkusinski for discussions.

[1] M. H. Weiler, in *Semiconductors and Semimetals*, edited by R. K. Willardson and A. C. Beer (Academic, New York, 1981), Vol. 16, p. 119.
[2] D. Bimberg, M. Grundmann, and N. N. Ledentsov, *Quantum Dot Heterostructures* (Wiley, New York, 1999).
[3] M. Bayer, A. Kuther, A. Forchel, A. Gorbunov, V. B. Timofeev, F. Schäfer, J. P. Reithmaier, T. L. Reinecke, and S. N. Walck, Phys. Rev. Lett. **82**, 1748 (1999); M. Bayer, A. Kuther, F. Schäfer, J. P. Reithmaier, and A. Forchel, Phys. Rev. B **60**, R8481 (1999).
[4] S. J. Sun and Y.-C. Chang, Phys. Rev. B **62**, 13631 (2000).
[5] I. Vurgaftman and J. R. Meyer, Phys. Rev. B **64**, 245207 (2001).
[6] W. Sheng and P. Hawrylak, Phys. Rev. B **73**, 125331 (2006).
[7] A. Babinski, G. Ortner, S. Raymond, M. Potemski, M. Bayer, W. Sheng, P. Hawrylak, Z. Wasilewski, S. Fafard, and A. Forchel, Phys. Rev. B **74**, 075310 (2006).
[8] O. Stier, Ph.D. thesis, Berlin Studies in Solid State Physics Vol. 7 (W&T, Berlin, 2000).
[9] M. Grundmann, *Nano-Optoelectronic: Concepts, Physics and Devices* (Springer, Berlin, 2002).
[10] W. Sheng, S.-J. Cheng, and P. Hawrylak, Phys. Rev. B **71**, 035316 (2005).
[11] A. V. Nenashev, A. V. Dvurechenskii, and A. F. Zinovieva, Phys. Rev. B **67**, 205301 (2003).
[12] T. Nakaoka, T. Saito, J. Tatebayashi, and Y. Arakawa, Phys. Rev. B **70**, 235337 (2004); T. Nakaoka, T. Saito, J. Tatebayashi, S. Hirose, T. Usuki, N. Yokoyama, and Y. Arakawa, *ibid.* **71**, 205301 (2005).
[13] U. Woggon, *Optical Properties of Semiconductor Quantum Dots*, Springer Tracts in Modern Physics Vol. 136 (Springer, Berlin, 1996).
[14] L. G. C. Rego, P. Hawrylak, J. A. Brum, and A. Wojs, Phys. Rev. B **55**, 15694 (1997).
[15] W. Sheng and J.-P. Leburton, Phys. Status Solidi B **237**, 394 (2003).
[16] N. J. Traynor, R. T. Harley, and R. J. Warburton, Phys. Rev. B **51**, 7361 (1995); N. J. Traynor, R. J. Warburton, M. J. Snelling, and R. T. Harley, *ibid.* **55**, 15701 (1997).
[17] A. Kuther, M. Bayer, A. Forchel, A. Gorbunov, V. B. Timofeev, F. Schäfer, and J. P. Reithmaier, Phys. Rev. B **58**, R7508 (1998).
[18] E. D. Minot, Yuval Yaish, V. Sazonova, and P. L. McEuen, Nature (London) **428**, 536 (2004).
[19] C. E. Pryor and M. E. Flatté, Phys. Rev. Lett. **96**, 026804 (2006).